Macromolecules

COMMUNICATION TO THE EDITOR

pubs.acs.org/Macromolecules

Nanomechanical Mapping on the Deformed Poly(ε-caprolactone)

Hao Liu, So Fujinami, Dong Wang, Ken Nakajima, and Toshio Nishi*

WPI Advanced Institute for Materials Research, Tohoku University, Sendai 980-8577, Japan

Supporting Information

Semicrystalline polymers are hierarchically structured materials. The microstructure texture and the molecular orientation level develop when a semicrystalline polymer is under shear or deformation, which in turn has an effect on the mechanical properties.[1] A low amount of orientation, as presented in thick extruded samples, does not have a significant effect on the mechanical behavior.[2] However, when the oriented structures happen all through the sample, like observed in high shear extruded samples, the anisotropic nature dominates the mechanical properties.[3] For this reason, several techniques such as necking or cold drawing for polymer films and fibers,[4−6] shear controlled orientation in injection molding (SCORIM),[7,8] etc., are used to create high degree of molecular orientation in order to enhance the mechanical properties. On the other hand, the necking phenomena occur when a ductile semicrystalline polymer is under deformation and lead to a highly oriented structure.[9] The deformation process is not homogeneous. Instead, two processes happen to the sample: one is the decreasing of transverse section, and another is the increasing of the lateral section, which makes it a complicated process. Accordingly, it is of great interest to investigate the oriented structure caused by stretching and its effect on the mechanical properties.[10,11]

In the literature, the deformation of semicrystalline polymers is widely studied by means of conventional characterization methods including small-angle X-ray scattering,[12−15] wide-angle X-ray diffraction,[14−16] and transmission electron microscopy.[14,17] However, the on-site morphology and mechanical properties in nanometer scale cannot be characterized simultaneously by these conventional methods, while techniques based on atomic force microscopy (AFM) offer the potential for imaging these material properties at the nanoscale.[18−22] Studies were focused on the development of quantitative micromechanical characterization, making it unique for detecting micromechanical surface properties.[23−25] The micromechanical mapping technology provides a new insight into fine details of polymer surfaces and interfaces, which was recently reviewed by Tsukruk.[26] In this work, we report quantitative investigation of both the on-site morphology and mechanical properties of stretched semicrystalline polymer samples by nanomechanical mapping. We use an AFM setup and nanomechanical mapping method as described in previous works.[27,28] Poly(ε-caprolactone) (PCL), a ductile semicrystalline polymer, is studied.

PCL films were prepared by a micro-twin-screw extruder. The films were then cut into dog-bone shape and uniaxially stretched at a fixed elongation of 700 ± 10% by a tensile tester. Afterward, both lateral sections of neat PCL and the necking part were cryosectioned and characterized on a commercial AFM system in force−volume (FV) mode for nanomechanical measurements. The obtained force−distance curves were analyzed using a procedure developed in our group.[29] Detailed experimental and analytical procedures are reported in the Supporting Information.

The deflection−displacement curves were directly acquired from the FV mode test, which can be converted to force−deformation curves by the simple relationships between deflection, displacement, and deformation.[30] Then, by applying JKR contact mechanics,[31] it is possible to calculate Young's modulus and adhesive energy. Figure 1 shows the typical force−deformation curve of neat and deformed PCL. The curve fitting against JKR contact is also superimposed in each case. The results show that JKR analysis of the withdrawing process fits well for both neat PCL and deformed PCL. Thus, it is proved that semicrystalline polymers are feasible to be studied by our nanomechanical mapping technique.

Young's moduli can be calculated from the obtained force−deformation curves. Accordingly, moduli map together with the moduli distribution histogram can be drawn. Figure 2 shows the topography and nanomechanical mapping of both neat and deformed PCL together with the moduli histogram. Neat PCL presents a relative uniform morphology and moduli mapping. Normal distribution of the moduli is shown in the moduli histogram. The average value of the calculated Young's modulus is 203 ± 24 MPa, which is larger than 124 ± 14 MPa calculated from uniaxial tensile test. The possible explanation for this phenomenon is that the moduli calculated from tensile test is the macroscopic value, which is affected by flaws among the polymer matrix, whereas the moduli calculated by nanomechanical measurement are in microscale and prevent the effect of imperfection. The topography of the lateral section of necking part shows obvious orientation along the tensile direction; similar morphology was reported in deformed polypropylene[25,32] and polyamide[33] matrix. The necking process is a heterogeneous deformation and results in fibrillar structure. The cryo-microtome process was supposed to make the cross sections in perfect plane. However, oriented height fluctuation can also be seen duo to the uneven fibrillar structure. Moreover, slight relaxation of the oriented nanofibrils might also contribute to the height difference.

More detailed topography of the necking part can be seen from the moduli map also shown in Figure 2. The surface topology is filled with nanofibrils, which are oriented along the tensile direction. Histograms of the moduli show a wider dispersion of moduli in the case of deformed PCL. The nanofibrils have

Received: January 4, 2011
Revised: February 27, 2011
Published: March 18, 2011

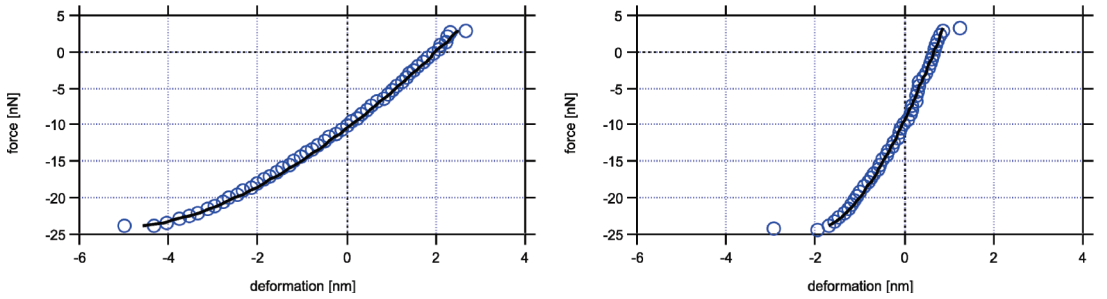

Figure 1. Force−deformation curve of both neat (left) and stretched (right) of PCL.

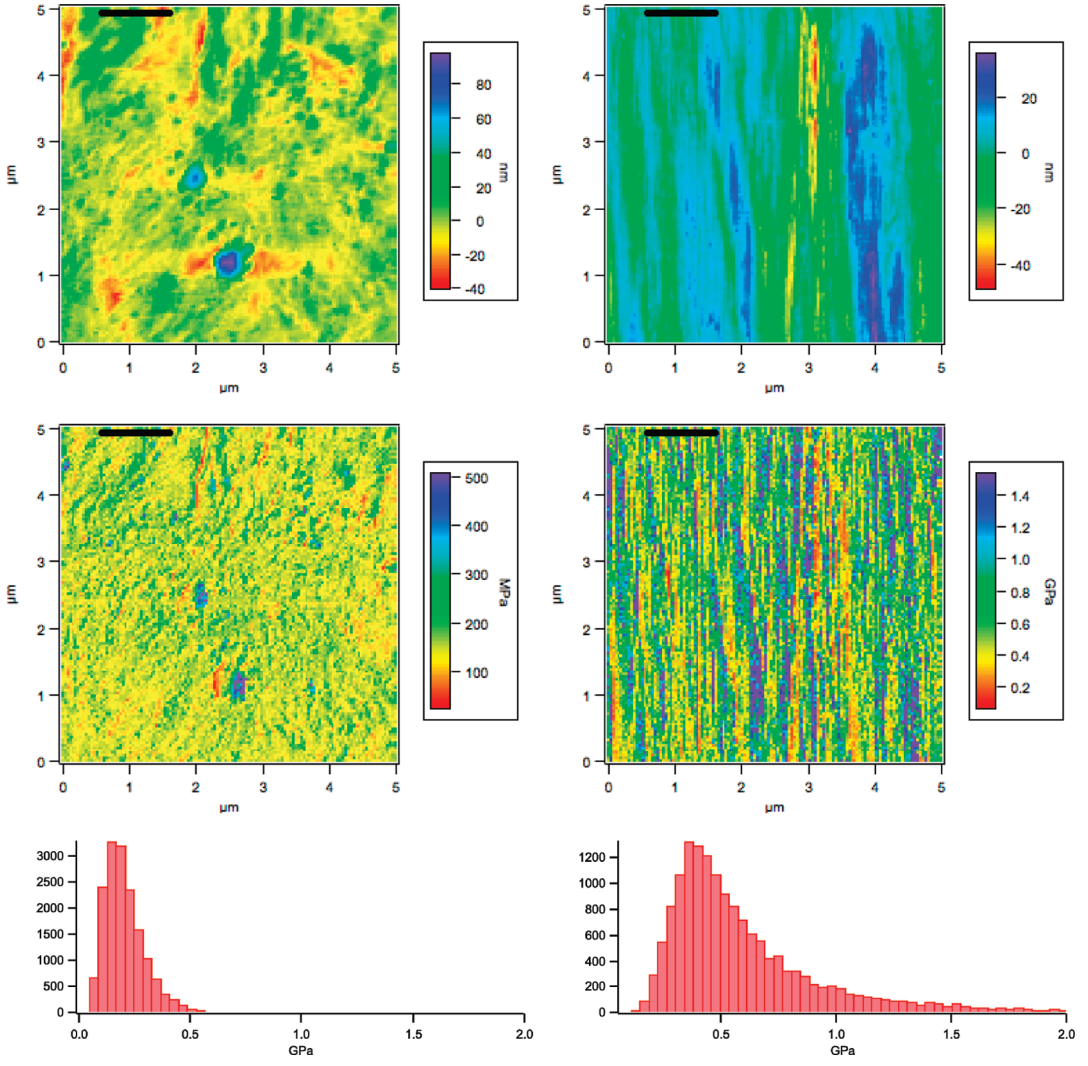

Figure 2. Topography and nanomechanical mapping of both neat (left) and stretched (right) of PCL. Black lines show the sections compared in Figure 3.

higher moduli and make the moduli distribution peak widened to the higher direction. Consequently, the necking parts have an average Young's modulus higher than neat PCL matrix. The average Young's modulus of the stretched PCL is 903 ± 121 MPa, whereas the value calculated form uniaxial tensile test of the necking park is 727 ± 160 MPa. The Young's modulus calculated by our nanomechanical mapping is comparable with their microscopic mechanical test result and provides a good method to quantitatively evaluate the mesoscopic mechanical properties of materials. However, it must be kept in mind that the moduli calculated might be affected by parameters such as deflection sensitivity, tip radius, etc., which may change during the characterization. Besides, the cryo-microtome processing and slight relaxation after microtoming might also have an effect on the calculated Young's moduli. The sections marked by black lines in Figure 2 are compared in Figure 3. The shape of nanofibrils with

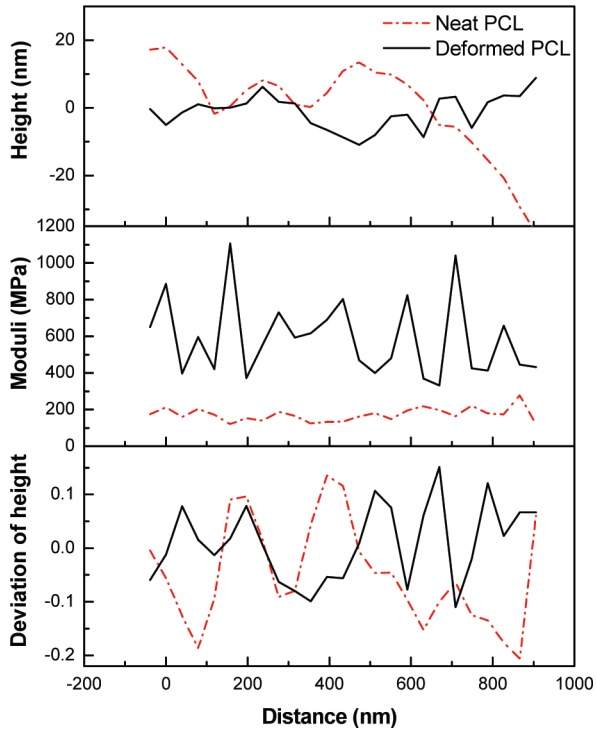

Figure 3. Section comparison of the height and Young's moduli of both neat and deformed PCL.

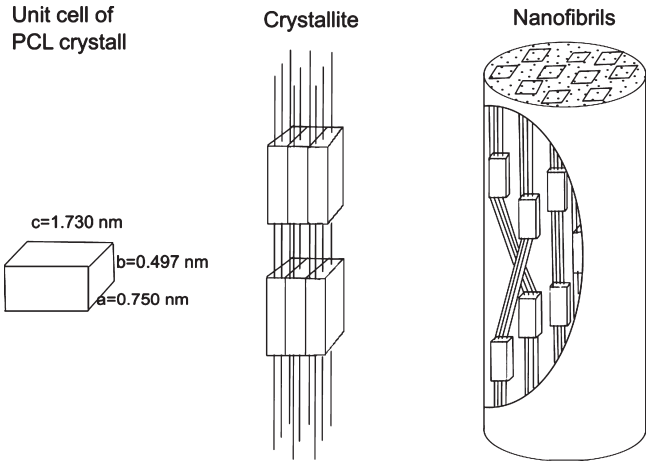

Figure 4. Schematic of the fibrillar structure of deformed PCL (the size of unit cell of PCL is calculated by Bittiger[36]).

higher moduli can be distinguished clearly with width of about 15−40 nm, very similar to 20−40 nm reported by Koike.[32]

The slope of the surface may cause false calculation of the Young's moduli. It is possible that the moduli difference is introduced by the height fluctuations of the sample surface. Accordingly, the section moduli and height in the same small fraction of the mapping, which are marked by black lines in Figure 2, were selected and compared in Figure 3. Results show that to some extent the calculated moduli are affected by the morphology, However, not all the peaks in the moduli map have corresponding peaks in the slope of the height map. The height fluctuations of neat PCL are even larger than deformed PCL while shows more uniform Young's moduli distribution. Consequently, the calculated Young's moduli are not directly affected by the height fluctuations and can be trusted.

On the basis of the nanomechanical mapping and combined with existing studies on the deformation behavior of PCL,[34] the orientated hierarchical structure and its microscopic mechanical property in the necking part are revealed, as shown in Figure 4. Fibrillar structure is attributed to the heterogeneous deformation of the lamellar. In the process of lamellar to fibrillar transition, intralamellar slips of the crystalline blocks were activated at low deformations, followed by stress-induced fragmentation and a recrystallization process.[35] In the high strain, heterogeneous intralamellar slip results in the formation of both orientations and entanglements of the nanofibrils, which is harder than neat polymer matrix and shows higher Young's modulus.

In conclusion, quantitative nanomechanical measurements were carried out on the neat and deformed PCL. Both the topography and Young's moduli mapping of the lateral section were obtained and compared. The lateral surface of necked part shows typical fibrillar structure, and the moduli mapping confirms the existence of nanofibrils. The nanofibrils are in the range of 15−40 nm in diameter and have much higher moduli of 903 ± 121 MPa than 203 ± 24 MPa for neat PCL matrix. The calculated microscopic moduli for neat and deformed PCL are comparable to the macroscopic value 727 ± 160 and 124 ± 14 MPa, respectively. Our data analysis procedure is feasible to get credible microscopic Young's moduli. The method will be useful to study the structure−property relationship of polymers as well as polymer nanocomposites.

■ ASSOCIATED CONTENT

Supporting Information. Detailed experimental and analytical procedures. This material is available free of charge via the Internet at http://pubs.acs.org.

■ REFERENCES

(1) Ward, I. M. *Structure and Properties of Oriented Polymers*; Chapman & Hall: London, 1997.
(2) Schrauwen, B. A. G.; Govaert, L. E.; Peters, G. W. M.; Meijer, H. E. H. *Macromol. Symp.* **2002**, *185*, 89.
(3) Southern, J. H.; Porter, R. S. *J. Appl. Polym. Sci.* **1970**, *14* (9), 2305.
(4) Vincent, P. I. *Polymer* **1960**, *1* (1), 7.
(5) Li, J. X.; Cheung, W. L. *Polymer* **1998**, *39* (26), 6935.
(6) Allison, S. W.; Ward, I. M. *Br. J. Appl. Phys.* **1967**, *18* (8), 1151.
(7) Ogbonna, C. I.; Kalay, G.; Allan, P. S.; Bevis, M. J. *J. Appl. Polym. Sci.* **1995**, *58* (11), 2131.
(8) Reis, R. L.; Mendes, S. C.; Cunha, A. M.; Bevis, M. J. *Polym. Int.* **1997**, *43* (4), 347.
(9) Leonov, A. I. *Int. J. Solids Struct.* **2002**, *39* (24), 5913.
(10) White, J. L.; Dharod, K. C.; Clark, E. S. *J. Appl. Polym. Sci.* **1974**, *18* (9), 2539.
(11) Jin, L.; Bower, C.; Zhou, O. *Appl. Phys. Lett.* **1998**, *73* (9), 1197.
(12) Jiang, Z. Y.; Tang, Y. J.; Men, Y. F.; Enderle, H. F.; Lilge, D.; Roth, S. V.; Gehrke, R.; Rieger, J. *Macromolecules* **2007**, *40* (20), 7263.
(13) Tang, Y. J.; Jiang, Z. Y.; Men, Y. F.; An, L. J.; Enderle, H. F.; Lilge, D.; Roth, S. V.; Gehrke, R.; Rieger, J. *Polymer* **2007**, *48* (17), 5125.
(14) Schrauwen, B. A. G.; Von Breemen, L. C. A.; Spoelstra, A. B.; Govaert, L. E.; Peters, G. W. M.; Meijer, H. E. H. *Macromolecules* **2004**, *37* (23), 8618.
(15) Koerner, H.; Kelley, J. J.; Vaia, R. A. *Macromolecules* **2008**, *41* (13), 4709.
(16) Lima, M. F. S.; Vasconcellos, M. A. Z.; Samios, D. *J. Polym. Sci., Polym. Phys.* **2002**, *40* (9), 896.

(17) Bartczak, Z.; Cohen, R. E.; Argon, A. S. *Macromolecules* **1992**, *25* (18), 4692.
(18) Sahin, O.; Quate, C. F.; Solgaard, O. *Phys. Rev. B* **2004**, *69*, 165416.
(19) Overney, R. M.; Meyer, E.; Frommer, J.; Guentherodt, H. J.; Fujihira, M.; Takano, H.; Gotoh, Y. *Langmuir* **1994**, *10* (4), 1281.
(20) Schönherr, H.; Beulen, M. W. J.; Bügler, J.; Huskens, J. ; van Veggel, F. C. J. M.; Reinhoudt, D. N.; Julius Vancso, G. *J. Am. Chem. Soc.* **2000**, *122* (20), 4963.
(21) Chizhik, S. A.; Huang, Z.; Gorbunov, V. V.; Myshkin, N. K.; Tsukru., V. V. *Langmuir* **1998**, *14* (10), 2606.
(22) Tsukruk, V. V.; Sidorenko, A.; Gorbunov, V. V.; Chizhik, S. A. *Langmuir* **2001**, *17* (21), 6715.
(23) Tsukruk, V. V.; Huang, Z. *Polymer* **2000**, *41* (14), 5541.
(24) Sahin, O.; Magonov, S.; Su, C.; Quate, C. F.; Solgaard, O. *Nanotechnology* **2007**, *2*, 507.
(25) Magonov, S. N.; Sheiko, S. S.; Deblieck, R. A. C.; Moller, M. *Macromolecules* **1993**, *26* (6), 1380.
(26) McConneya, M. E.; Singamanenia, S.; Tsukruk, V. V. *Polym. Rev.* **2010**, *50* (3), 235.
(27) Wang, D.; Fujinami, S.; Nakajima, K.; Nishi, T. *Macromolecules* **2010**, *43* (7), 3169.
(28) Wang, D.; Fujinami, S.; Liu, H.; Nakajima, K.; Nishi, T. *Macromolecules* **2010**, *43* (13), 5521.
(29) Nukaga, H.; Fujinami, S.; Watabe, H.; Nakajima, K.; Nishi, T. *Jpn. J. Appl. Phys.* **2005**, *44* (7b), 5425.
(30) Bhowmick, A. K. *Current Topics in Elastomers Research*; CRC Press: Boca Raton, FL, 2008; Chapter 21.
(31) Johnsonm, K. L.; Kendall, K.; Roberts, A. D. *Proc. R. Soc. London., Ser. A* **1971**, *324*, 301.
(32) Koike, Y.; Cakmak, M. *J. Polym. Sci., Polym. Phys.* **2006**, *44* (6), 925.
(33) Ferreiro, V.; Pennec, Y.; Seguela, R.; Coulon, G. *Polymer* **2000**, *41* (4), 1561.
(34) Men, Y.; Strobl, G. *Macromolecules* **2003**, *36* (6), 1889.
(35) Jiang, Z.; Tang, Y.; Rieger, J.; Enderle, H. F.; Lilge, D.; Roth, S. V.; Gehrke, R.; Heckmann, W.; Men, Y. *Macromolecules* **2010**, *43* (10), 4727.
(36) Bittiger, H.; Marchess, Rh; Niegisch, W. D. *Acta Crystallogr., Sect. B: Struct. Sci.* **1970**, *26*, 1923.